ELSEVIER

Catalysis Today 48 (1999) 199–209

CATALYSIS TODAY

The simulated moving-bed reactor for production of bisphenol A

Motoaki Kawase, Yasunobu Inoue, Takushi Araki, Kenji Hashimoto*

Department of Chemical Engineering, Kyoto University, Kyoto 606-8501, Japan

Abstract

Bisphenol A was produced from acetone and phenol over an ion-exchange resin catalyst at 50–90°C. Phenol was used as solvent. The reaction proceeded under the excess phenol condition. The reaction rate was proportional to the acetone concentration in the initial period of the reaction. After the acetone conversion exceeded approximately 50%, the reaction rate became lower than expected by the first-order reaction rate. This was ascribed to water adsorption onto the resin. Batch adsorption and breakthrough experiments showed that water was adsorbed approximately seven times stronger than acetone and that bisphenol A was not adsorbed. Using the reaction rate equation for bisphenol A production, the adsorption isotherms and overall mass transfer coefficients of the components, the numerical simulation of the 3-zone-type simulated moving-bed reactor was carried out. High resin flow rate was required in order to remove water out of the reaction zone, and a high liquid flow rate was also required to desorb water from the resin in the recovery zone. As far as the flow rates were set appropriately, water was successfully removed to prevent the catalyst deactivation and the long-term stable production of BPA was allowed.

Keywords: Simulated moving-bed reactor; Numerical simulation; Bisphenol A; Ion-exchange resin catalyst

1. Introduction

Bisphenol A [2,2-bis(4-hydroxyphenyl) propane, BPA] is an important chemical for producing a number of engineering resins. BPA (C) is produced from acetone (A) and phenol (B) with a by-product, water (D), as follows:

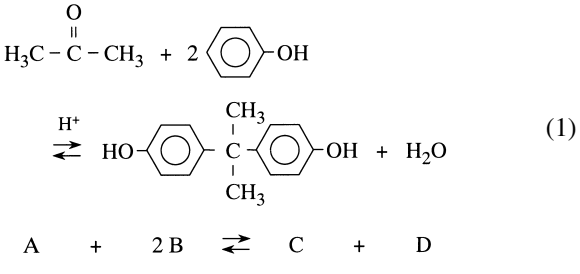

(1)

A + 2 B ⇄ C + D

*Corresponding author.

Although the reaction is reversible, a high acetone conversion around 95% is obtained by employing phenol as solvent in an industrial production [1]. A proton-type ion-exchange resin catalyst has been recently used in packed-bed reactors, instead of mineral acid catalysts. By employing the ion-exchange resin catalyst, a number of problems such as removal of the homogeneous catalyst from the product and corrosion by the mineral acid, were solved. However, the adsorption of by-produced water decreases the catalytic activity of the resin. As water spreads towards the outlet, the acetone conversion decreases. This accumulation of water prevents a long-term operation of the process. In order to allow a stable operation, water has to be removed continuously from the reactor. A simultaneous reaction and separation process is one of the possible solutions.

0920-5861/99/$ – see front matter
PII: S0920-5861(98)00374-5

Among several reaction–separation processes, the chromatographic reactor is employed in this study, since the proton-type ion-exchange resin acts not only as catalyst but also as adsorbent. Especially, the simulated moving-bed reactor was investigated. It has been successfully applied to several reactions on a laboratory scale. The liquid-phase reactions, such as esterification of acetic acid with β-phenethyl alcohol [2], esterification of acetic acid with ethanol [3], and saccharification of starch to maltose [4], as well as the gas-phase reactions, such as hydrogenation of methylbenzene [5] and oxidative coupling of methane [6], have been carried out.

The simulated moving bed consists of a number of columns, which are connected in series. As shown in Fig. 1, by switching the liquid inlet and outlet positions column by column in a certain interval T_S, an intermittent resin flow in the direction opposite to the liquid flow is created. From the viewpoint of the liquid

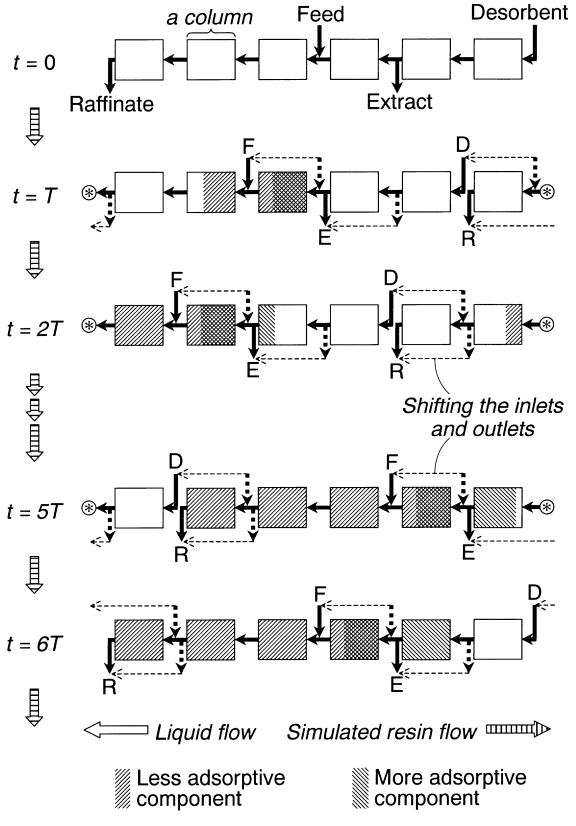

Fig. 1. Concept of the simulated moving bed.

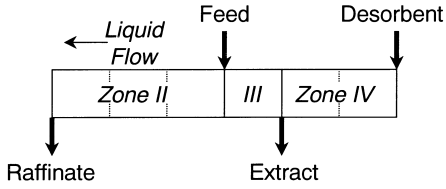

Fig. 2. Three-zone-type simulated moving-bed reactor.

inlets and outlets, the more adsorptive component migrates with the resin, whereas the less adsorptive component migrates with the liquid. The two components are thus separated continuously.

Fig. 2 shows a schematic illustration of the 3-zone-type simulated moving-bed reactor. The simulated moving bed is divided into zones of different numbers of columns by the liquid inlets and outlets. In this example, zones II, III, and IV consist of 3, 1, and 2 columns, respectively. A 4-zone-type simulated moving bed, which has zone I in order to purify the desorbent, is often used. Zone I is omitted in this system, since BPA is little adsorbed as described later. As the columns are connected in a circular arrangement, the column that leaves zone IV is recycled to zone II.

Acetone is fed between zones II and III, whereas phenol is fed as the desorbent. The condensation reaction takes place near the feed point, to produce BPA and water. The resin flow removes adsorbed water out of the reaction zones. Water is desorbed by a high flow rate of desorbent in zone IV, and withdrawn between zones III and IV as extract. BPA is obtained from the exit of zone II as raffinate.

In this study, the reaction rate of BPA production catalyzed by the ion-exchange resin is formulated. The adsorption isotherms and overall volumetric mass transfer coefficients of acetone, BPA and water are measured. The numerical simulation is carried out using the measured parameters to investigate the application of the simulated moving-bed reactor to the BPA production.

2. Experimental

2.1. Batch reaction experiments

Proton-type ion-exchange resin, Amberlyst 31 (Rohm and Haas) was used as catalyst. Amberlyst

31 was designed as heterogeneous acid catalyst for organic reactions, having a medium level of cross-linking. The average diameter is 0.58 mm, and the acid site concentration is 4.8 mol/kg. Reactants were acetone and phenol, and phenol was also used as solvent. Prior to each experiment, the ion-exchange resin was presoaked with phenol, and the reaction experiment began with addition of acetone.

The batch reaction experiments were carried out with about 10 g of the catalyst and 100 cm^3 of acetone–phenol mixture at 50–90°C. Mole ratio of phenol to acetone was approximately 12, unless otherwise noted. The solution was stirred so fast that the effect of mass transfer was not observed. The solution was sampled with a micro syringe in a certain interval for analysis. Concentrations of acetone and BPA were measured using an HPLC with a UV detector (ShimadzuSPD-6A). Water concentration was measured using a Karl–Fischer moisture titrator (Kyoto Electronics MKC-210).

2.2. Batch adsorption experiments

Adsorption of BPA and water was measured in batch adsorption experiments in a shaking bath at 70°C. The adsorbent was 1 g of Amberlyst 31, and the solvent was 25 cm^3 of phenol. The resin was added to a certain concentration of adsorbate solution. The change in adsorbate concentration was measured until a steady state was reached. Concentrations were measured in the same manner as in the batch reaction experiments. The adsorbed amount was calculated from the decrease in the concentration in the solution.

The obtained adsorption isotherm was fitted with a Langmuir-type equation

$$q_k = m_k C_k^* / (1 + K_k C_k^*). \tag{2}$$

The adsorption parameters m_C and K_C of BPA and m_D, K_D of water were determined in the respective batch adsorption experiments. No batch adsorption experiment for acetone was carried out, since acetone would react with phenol in the presence of the resin.

2.3. Breakthrough experiments

The breakthrough curves of BPA and water were measured at 70°C using a stainless steel column with an inner diameter of 1.0 and 30 cm in length, packed with Amberlyst 31. Packing density was ρ=958 kg/m^3, and the bed porosity was ϵ_b=0.413. The liquid flow rate was 2.0 cm^3/min. The resin was saturated with a certain concentration C_0 of adsorbate. Then the feed concentration was changed stepwise to C_1. The obtained breakthrough curves were fitted with the results of numerical simulation.

In the simulation model, the mass balance equations for adsorbate are expressed as follows:

$$\epsilon_b \frac{\partial C}{\partial t} = -v \frac{\partial C}{\partial z} - K_f a_v (C - C^*), \tag{3}$$

$$(1 - \epsilon_b) \frac{dq}{dC^*} \frac{dC^*}{dt} = K_f a_v (C - C^*), \tag{4}$$

where C is the concentration of adsorbate in the liquid phase, C^* the equilibrium concentration to the adsorbed amount q, v the superficial liquid velocity, and $K_f a_v$ is the overall volumetric liquid–solid mass transfer coefficient. The initial and boundary conditions are as follows:

$$C = C^* = C_0, \quad 0 \le z \le L_a, \quad t = 0, \tag{5}$$

$$C = C_1, \quad z = 0, \quad t > 0. \tag{6}$$

These equations were converted into finite difference equations and solved numerically. dq/dC^* was assumed to be the same as determined in the batch adsorption experiments. The overall volumetric liquid–solid mass transfer coefficient $K_f a_{v,D}$ of water was determined by finding a minimum of the sum of squared errors between the calculated and measured concentrations.

2.4. Fixed-bed reaction experiments

Fixed-bed reaction experiments were carried out at 70°C in the same apparatus as in the breakthrough experiments. The mole ratio of acetone to phenol was kept approximately 1:12. The total liquid flow rate was 2.0 cm^3/min.

When acetone was fed to the column, the condensation reaction took place. In this case, the numerical simulation of the fixed-bed reactor was carried out. The mass balance equations were the same as in the numerical simulation of the simulated moving-bed reactor described later Eqs. (16)–(19). The initial and boundary conditions were expressed by Eqs. (5) and (6), where C_0=0.

Because of the acetone concentration dependency of the reaction rate as described later, the following adsorption isotherm of acetone was assumed:

$$q_A = m_A C_A^* / (1 + K_D C_D^*). \quad (7)$$

By finding a minimum of the sum of squared errors between the calculated and measured acetone and BPA concentrations, the optimal values of m_A in Eq. (7) and overall volumetric mass transfer coefficient $K_f a_{v,A}$ of acetone were determined.

3. Experimental results and discussion

3.1. Reaction kinetics

Fig. 3 shows the results of the batch reaction experiments carried out at an acetone-to-phenol mole ratio of 1:12. At each temperature, the acetone concentration decreased exponentially in the low-conversion range. This indicates that the reaction rate was first-order with respect to the acetone concentration in the initial period of reaction. The apparent first-order reaction rate constants were calculated from the slope of the lines drawn in Fig. 3. Fig. 4 shows the apparent first-order reaction rate constants measured at different concentrations of acetone. The rate constants were almost constant in the concentration range of this study. This proves the first-order reaction rate law.

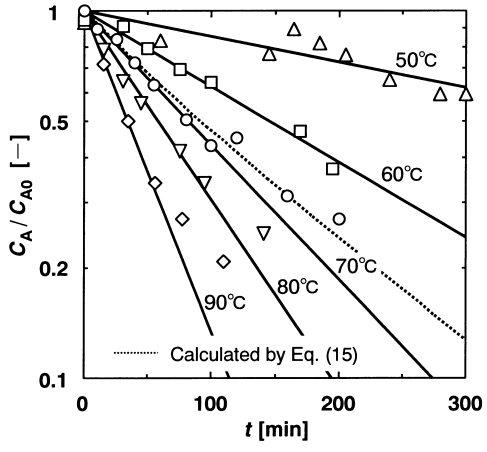

Fig. 3. Transient changes in the acetone concentration (batch reaction experiments).

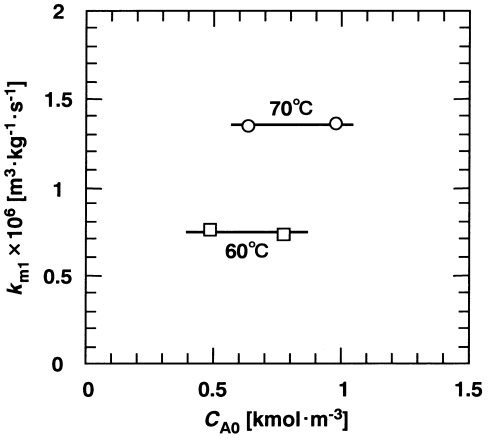

Fig. 4. Dependency of the apparent first-order reaction rate constants on the acetone concentration.

The observed first-order reaction rate constants were plotted against the reciprocal of the reaction temperature in Fig. 5. The data points were correlated with the following equation

$$k_{ml} = 1470 \exp(-59\,900/RT)[\mathrm{m^3\,kg^{-1}\,s^{-1}}]. \quad (8)$$

The apparent activation energy was 59.9 kJ/mol in the temperature range 50–90°C. Reinicker and Gates [7] reported the reaction rates of BPA production over

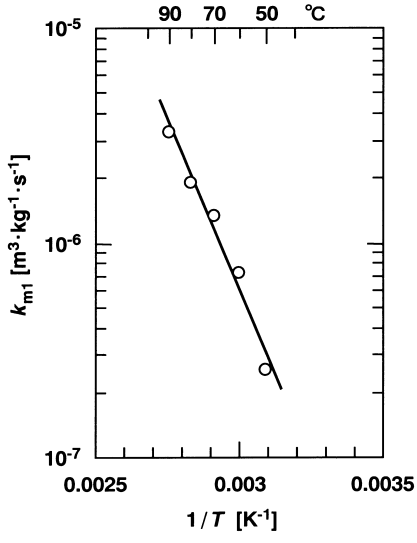

Fig. 5. Arrhenius plot of the apparent first-order reaction rate constants.

another ion-exchange resin, Dowex 50W. Their results showed almost the same value of the activation energy.

As shown in Fig. 3, after the acetone conversion exceeded around 0.5, the reaction rate decreased gradually. This was ascribed to the adsorption of water produced. Water was strongly adsorbed on the acidic sites, and inhibited the catalytic reaction. Hence, the reaction rate decreased as the water concentration increased.

When the carbonium ion mechanism, which accounts for a lot of acid-catalyzed condensation reactions [7,8], is assumed, the reaction mechanism is expressed as follows:

$$\mathrm{A} + \sigma \underset{k_{-\mathrm{A}}}{\overset{k_{\mathrm{A}}}{\rightleftarrows}} \mathrm{A}\sigma, \quad K_{\mathrm{A}} = k_{\mathrm{A}}/k_{-\mathrm{A}}, \tag{9}$$

$$\mathrm{A}\sigma + \mathrm{B} \underset{k_{-1}}{\overset{k_1}{\rightleftarrows}} M\sigma, \quad K_1 = k_1/k_{-1}, \tag{10}$$

$$M\sigma + \mathrm{B} \underset{k_{-2}}{\overset{k_2}{\rightleftarrows}} \mathrm{C} + \mathrm{D}\sigma, \tag{11}$$

$$\mathrm{D}\sigma \underset{k_{\mathrm{D}}}{\overset{k_{-\mathrm{D}}}{\rightleftarrows}} \mathrm{D} + \sigma, \quad K_{\mathrm{D}} = k_{\mathrm{D}}/k_{-\mathrm{D}}. \tag{12}$$

Assuming reaction (11) to be the rate-determining step, the overall reaction rate is expressed as follows:

$$-r_{\mathrm{Am}} = \frac{k_2 K_1 K_{\mathrm{A}} C_{\mathrm{A}}^* C_{\mathrm{B}}^{*2} - k_{-2} K_{\mathrm{D}} C_{\mathrm{C}}^* C_{\mathrm{D}}^*}{1 + K_{\mathrm{A}} C_{\mathrm{A}}^* (1 + K_1 C_{\mathrm{B}}^*) + K_{\mathrm{D}} C_{\mathrm{D}}^*}, \tag{13}$$

where superscripts $*$ denote that the adsorption equilibrium is reached. Under the excess phenol condition, the following rate equation is derived:

$$-r_{\mathrm{Am}} = \frac{k_{\mathrm{m1}} C_{\mathrm{A}}^*}{1 + K'_{\mathrm{A}} C_{\mathrm{A}}^* + K_{\mathrm{D}} C_{\mathrm{D}}^*}, \tag{14}$$

where $k_{\mathrm{m1}} = k_2 K_1 K_{\mathrm{A}} C_{\mathrm{B}}^{*2}$ and $K'_{\mathrm{A}} = K_{\mathrm{A}}(1 + K_1 C_{\mathrm{B}}^*)$. Since the inhibition effect of acetone was negligibly small under the conditions of this study as shown in Fig. 4, Eq. (14) is simplified to as follows:

$$-r_{\mathrm{Am}} = k_{\mathrm{ml}} C_{\mathrm{A}}^* / (1 + K_{\mathrm{D}} C_{\mathrm{D}}^*). \tag{15}$$

At the beginning of the reaction, the water concentration was so low that the reaction rate became first-order with respect to the acetone concentration. As the reaction proceeded to increase the water concentration, the inhibition effect of water reduced the reaction rate. The adsorption equilibrium constant K_{D} of water was measured in the adsorption experiments as described later. The broken line in Fig. 3 shows the result calculated by Eq. (15), which is in better agreement with the experimental result than the first-order reaction rate equation.

3.2. Batch adsorption experiments – adsorption isotherms of BPA and water

The batch adsorption of BPA was carried out at an initial concentration of 0.31 kmol/m^3. The BPA concentration in the solution was constant within an error of 4% even after 1080 min. BPA was little adsorbed on Amberlyst 31.

The batch adsorption experiments of water were carried out at initial water concentrations of 0.28–1.35 kmol/m^3. The water concentration in the solution decreased by 23–32%, and reached the equilibrium concentration approximately in 30 h. Using the concentration after 40 h adsorption, the equilibrium amount adsorbed was calculated. Fig. 6 shows the obtained adsorbed amount q_{D} against the equilibrium concentration C_{D}^* in the liquid phase. By finding the slope and intercept of a straight line on a plot of $1/q_{\mathrm{D}}$ versus $1/C_{\mathrm{D}}^*$, the adsorption parameters, m_{D} and K_{D}, were determined. They are listed in Table 1.

3.3. Breakthrough experiments – overall mass transfer coefficient of water

The breakthrough experiment of BPA was carried out at C_0=0, C_1=0.31 kmol/m^3. BPA was eluted out

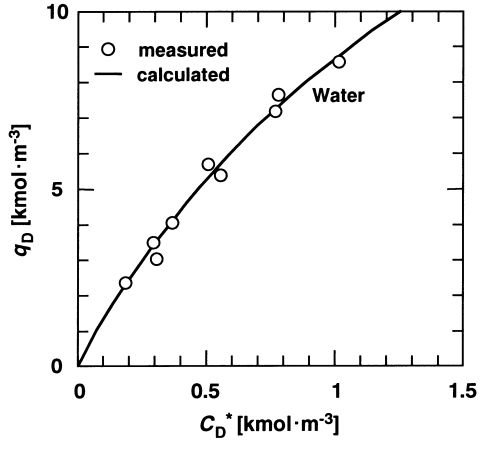

Fig. 6. Adsorption isotherm of water at 70°C.

Table 1
Adsorption isotherms and overall volumetric mass transfer coefficients

	Adsorption isotherm (q, C^* (mol/m^3))	$K_f a_v$[a] (min^{-1})
Acetone	$q_A = 1.9C_A^*/(1 + K_D C_D^*)$	0.32
Water	$q_D = 13.4C_D^*/(1 + K_D C_D^*)$	3.42

K_D=5.44×10^{-4} m^3/mol.
[a]Measured at v=2.5 cm/min.

without any delay due to adsorption. It was proved that BPA was not adsorbed on Amberlyst 31.

The breakthrough experiments of water were carried out at C_0=0, C_1=0.21 kmol/m^3 and at C_0=0.21, C_1=0.72 kmol/m^3. The observed retention time of water was in good agreement with that expected from the results of the batch adsorption experiments. The overall mass transfer coefficient $K_f a_{v,D}$ of water was determined in the breakthrough experiments, and is listed in Table 1.

3.4. *Fixed-bed reaction experiments – adsorption isotherm and overall mass transfer coefficient of acetone*

Fig. 7 shows the results of the fixed-bed reaction experiment. The acetone concentration at the inlet was C_1=0.61 kmol/m^3, and the superficial liquid velocity was v=2.5 cm/min. The calculated concentrations are also shown in the figure. The reaction rate equation, the adsorption parameters, m_D and K_D, and the mass transfer coefficient $K_f a_{v,D}$ of water were taken from the results of the batch reaction and breakthrough experiments. The adsorption equilibrium and mass transfer coefficient of acetone were estimated from the experimental results of the fixed-bed reactor experiments shown in Fig. 7. Since the catalytic reaction rate was proportional to the acetone concentration and reduced by the water adsorption as shown in Fig. 4, it was assumed that the adsorption isotherm of acetone can be expressed by Eq. (7).

The adsorption parameter m_A and mass transfer coefficient $K_f a_{v,A}$ of acetone were determined by comparing the calculated and measured results. The optimal value of m_A in the acetone concentration range of 0–0.61 kmol/m^3 was 1.9. The adsorption isotherm equation and $K_f a_{v,A}$ are listed in Table 1. As shown in Fig. 7, the calculated concentration changes of acetone and BPA were in good agreement with the experimental results. Although the calculated water concentration change represented well the retention time of water, the absolute values of the calculated water concentration were not in good agreement with the experimental results. This suggests that $K_f a_{v,D}$ decreased in the presence of acetone or BPA. However, the value of $K_f a_{v,D}$ does not greatly influence the results of the numerical simulation of the simulated moving-bed reactor, as far as the adsorption isotherm is correct.

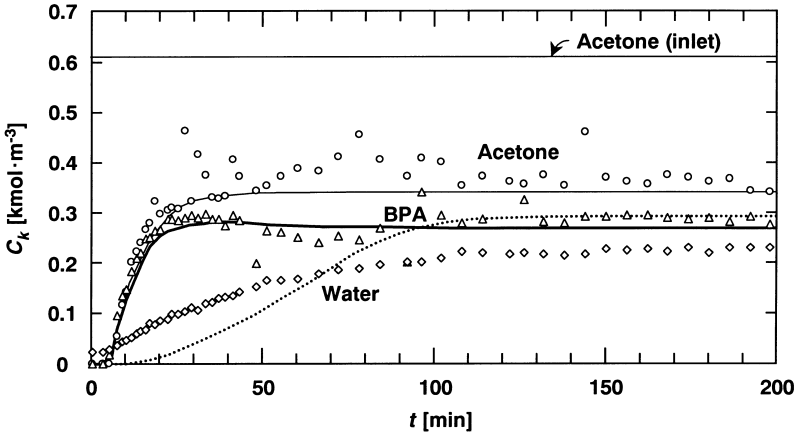

Fig. 7. Results of the fixed-bed reactor experiment. Keys represent the experimental results and lines are the calculated results: (——○——) acetone; (——Δ——) BPA; and (···◇···) water.

4. Numerical simulation of the simulated moving-bed reactor

4.1. Model description

Using the experimentally determined reaction rate equation, adsorption isotherms, and overall mass transfer coefficients, the numerical simulation of the simulated moving-bed reactor was carried out at 70°C. Since BPA is not adsorbed on the resin, the 3-zone-type simulated moving-bed reactor shown in Fig. 2 was taken into consideration.

The intermittent moving-bed model [2,9–11] was employed in this study. In this model, the simulated moving bed is not approximated to be a true moving bed, but is regarded as a fixed bed except at the moment of shifting the inlets and outlets of liquid. The mass balance equations of component k (=A, D) in zone n are expressed as follows:

Liquid phase:

$$\epsilon_b \frac{\partial C_k}{\partial t} = -v_n \frac{\partial C_k}{\partial z} - K_f a_{v,k}(C_k - C_k^*). \tag{16}$$

Adsorbed phase:

$$(1-\epsilon_b)\frac{dq_k}{dt} = K_f a_{v,k}(C_k - C_k^*) + \rho r_{k,m}, \tag{17}$$

where C_k is the concentration in the liquid phase, C_k^* the equilibrium concentration to the adsorbed amount q_k, v_n the superficial liquid velocity in zone n, and $r_{k,m}$ represents the catalytic reaction rate of component k. The overall volumetric coefficient $K_f a_v$ is introduced to describe the mass transfer. The dependence of $K_f a_v$ on the liquid velocity is ignored, since the value of $K_f a_v$ does not greatly influence the results of the numerical simulation of the simulated moving-bed reactor.

Since BPA is not adsorbed on the resin as described before, the reaction term is moved to the liquid phase equation as follows:

Liquid phase:

$$\epsilon_b \frac{\partial C_C}{\partial t} = -v_n \frac{\partial C_C}{\partial z} + \rho r_{Cm}. \tag{18}$$

Since the adsorption equilibrium of acetone is dependent on the adsorption of water, dq_k/dt must be calculated as follows:

$$\frac{dq_A}{dt} = \frac{\partial q_A}{\partial C_A^*}\frac{dC_A^*}{dt} + \frac{\partial q_A}{\partial C_D^*}\frac{dC_D^*}{dt}, \tag{19}$$

$$\frac{dq_D}{dt} = \frac{dq_D}{dC_D^*}\frac{dC_D^*}{dt}.$$

Equations in terms of C_k^* are derived from Eqs. (17) and (19).

The boundary conditions are as follows:

$$v_f C_{k,f} + v_{III} C_{k,III_{out}} = v_{II} C_{k,II_{in}}, \tag{20}$$

$$C_{k,IV_{out}} = C_{k,III_{in}}, \tag{21}$$

$$C_{k,IV_{in}} = 0, \tag{22}$$

where subscripts 'n_{in}' and 'n_{out}', respectively, represent the liquid inlet and outlet of zone n, and a subscript f represents the feed stream.

These equations are converted into the finite difference equations by Euler's scheme and solved numerically. Concentrations in the columns are calculated for a switching interval, and then the concentration distributions are shifted according to a column shift. This procedure is repeated until the steady-state concentration profiles are obtained.

4.2. Model parameters

The eight parameters, which control the behavior of the simulated moving-bed reactor, are listed in Table 2. L_a, n_{III}, n_{IV}, v_{II}, and v_{III} are fixed in the numerical simulation. The other parameters, T_S, n_{II}, and v_{IV}, are varied.

Feed is assumed to be undiluted acetone, and therefore the concentration C_{Af} of acetone in the feed stream is constant. The acetone feed rate in terms of unit cross-sectional area of a column is fixed as $v_f C_{Af}$=126 mol/(m^2 min). This rate is determined so

Table 2
Parameters governing the three-zone-type simulated moving-bed reactor

Column length	L_a
Switching interval	T_S
Number of columns in zone II	n_{II}
Number of columns in zone III	n_{III}
Number of columns in zone IV	n_{IV}
Liquid velocity in zone II	v_{II}
Liquid velocity in zone III	v_{III}
Liquid velocity in zone IV	v_{IV}

that the BPA production rate should be 50 000 t/year when an inner diameter of columns is 2 m.

The column length L_a is fixed to be 2 m. In order to prevent acetone from leaking in the extract stream, one column is required in zone III at least (cf. Fig. 1). Since acetone is weakly adsorbed, only one column is possible and n_{III} is fixed to be 1. n_{IV} is fixed to be 2, which was determined in the preliminary simulations so that the water fraction would be around 1% in the product except for solvent. n_{II} is varied in the range 1–6. These numbers of columns are realistic, since the total number of columns is preferred to be 3–10 in the industrial application.

v_{III} is determined so that the acetone-to-phenol ratio in zone II would be 1:12. v_{II} is a sum of v_{III} and v_f. Since the acetone feed rate is fixed, v_{II} and v_{III} are also constant: v_{II}=15.4 cm/min and v_{III}=14.4 cm/min. v_{IV} is varied in the range 14.5–86.7 cm/min. These velocities meet the space velocity range of 1–5 h^{-1} that is recommended by Rohm and Haas.

Switching time T_S is varied in the range 20–120 min. T_S has to be longer than several minutes when considering the industrial application.

Instead of T_S, n_{II}, and v_{IV}, three modified parameters, u_{II}/u_S, u_{IV}/u_S, and τ_{II}, are introduced for the reason of convenience. u_S is the resin velocity, defined as L_a/T_S. u_n is the liquid velocity of the equivalent true moving bed in zone n, defined as $v_n/\epsilon_b - u_S$. τ_{II} is the liquid residence time in zone II, defined as $L_a n_{II}/u_{II}$. The first aim of applying the simulated moving-bed reactor to the BPA production is to remove water out of the reaction zone continuously. This is achieved by sufficiently increasing the resin flow rate compared with the liquid flow rate so that water should migrate with the resin in zone II. This effect is mainly determined by the parameter, u_{II}/u_S. In addition, a sufficient liquid flow rate in zone IV is required in order to desorb water from the resin. This condition is represented by u_{IV}/u_S. If water is successfully removed out of the system, the acetone conversion and BPA yield are determined by the liquid residence time τ_{II} in zone II. The effects of these three parameters are investigated.

4.3. General results

Fig. 8(a) shows the typical calculated results of the steady-state concentration profiles in the simulated moving-bed reactor. Fig. 8(b) and (c) show the transient changes in concentrations in the raffinate and extract streams, respectively. It took about 400 min, or 15 times column shifts, to reach the steady state. As shown in Fig. 8(a), the reaction took place downstream of the feed point. BPA was obtained in the raffinate stream at a high yield of 99.5% and at high purity. Water distributed mainly in zone III and near the feed inlet in zone II. This indicates that produced water was adsorbed on the resin and successfully removed from the reaction zone by column shifts. The resin was regenerated in zone IV by desorbing

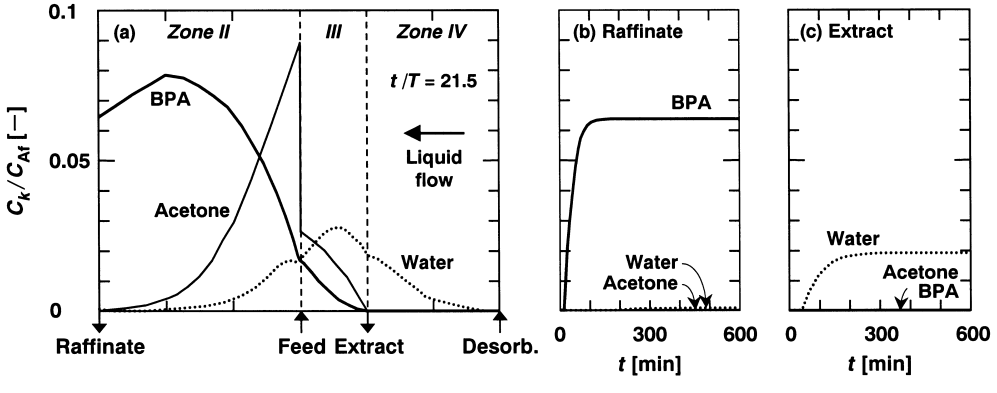

Fig. 8. Results of the simulated moving-bed reactor simulation: (a) steady-state concentration profiles; (b) transient concentration changes in the raffinate stream; (c) transient concentration changes in the extract stream. (τ_{II}=20.1 min; u_S=7.46 cm/min; u_{II}/u_S=4.0; u_{IV}/u_S=20.0; T_S=26.8 min; $v_f C_{Af}$=126 mol/(m^2·min)).

water. Since water was withdrawn continuously, the stable long-term operation was possible. Under the conditions of Fig. 8(a)–(c), BPA can be produced at a rate of 50 000 t/year, with a column diameter of 2 m.

4.4. Removal of water out of the reaction zone

Fig. 9 shows the effects of the resin velocity u_S on the acetone conversion and the water recovery. The water recovery is defined as the fraction of water obtained in the extract stream in the water production rate. u_S was only varied by changing the switching time T_S, while u_{IV}/u_S and v_{II} were fixed. τ_{II} was in inverse proportion to u_{II}, and τ_{II}=20.1 min at u_{II}/u_S=4.0.

As shown in Fig. 9, as the liquid–solid velocity ratio decreased, water was more effectively removed, and the acetone conversion increased. In order to obtain a conversion higher than 0.99, the liquid–solid velocity ratio was required to be less than 5.

Hashimoto and co-workers [9–11] proposed the β parameter defined as follows:

$$\beta_{k,n} = \epsilon_b u_n / [(1-\epsilon_b) u_S (\mathrm{d}q_k/\mathrm{d}C_k^*)_{\mathrm{average}}]. \quad (23)$$

When $\beta_{k,n}$ is less than 1, component k migrates with the resin in the simulated moving bed. Using the calculated average water concentration in zone II, $\beta_{D,II}$ became 1 when u_{II}/u_S=6.97. The acetone conversion was changed drastically at this point as shown in Fig. 9. This indicates that the β criterion is a minimum requirement even in designing a simulated moving-bed reactor process as well as a separation process.

4.5. Recovery of water in zone IV

The liquid velocity that could desorb water from the resin in zone IV was investigated. Fig. 10 shows the acetone conversion and the water recovery with respect to the liquid–solid velocity ratio u_{IV}/u_S in zone IV. Only u_{IV} was varied, while the other parameters, u_{II}, u_S, and τ_{II}, were fixed.

As the liquid velocity in zone IV decreased, water could not be desorbed in zone IV. Water adsorbed on the resin was transported to zone II by column shift. This reduced the acetone conversion. A liquid–solid velocity ratio higher than 20 was required in zone IV, to withdraw 99% of water in the extract stream. When

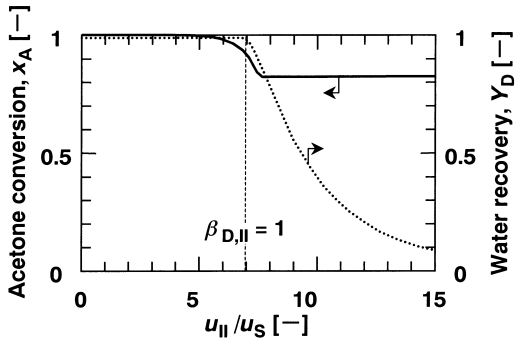

Fig. 9. Effect of the resin flow rate on removal of water out of the reaction zone: u_{IV}/u_S=20.0; v_{II}=15.4 cm/min.

u_{IV}/u_S=16.2, $\beta_{D,IV}$ became 1. The β parameter also gives a good criterion.

In order to reduce u_{IV}, u_S has to be lowered. However, a high u_S is required to remove water out of the reaction zone. The trade-off of these two requirements causes an optimal resin velocity u_S.

4.6. Residence time in the reaction zone

If the flow rates of solid and liquid in each zone are set appropriately, the inhibition effect of water is eliminated and the acetone conversion is determined only by the residence time in the reaction zone.

Fig. 11 shows the calculated results of the acetone conversion at different residence time τ_{II}. τ_{II} was varied by the number n_{II} of columns in zone II, while the other parameters, u_{II}, u_{IV}, and u_S, were fixed. The

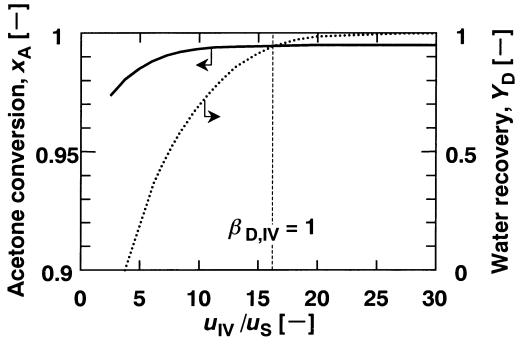

Fig. 10. Effect of the desorbent flow rate on recovery of water: u_{II}/u_S=4.0; τ_{II}=20.1 min.

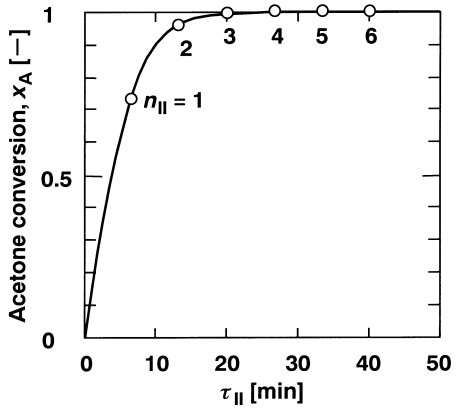

Fig. 11. Effect of the residence time in the reaction zone on the acetone conversion: u_{II}/u_S=4.0; u_{IV}/u_S=20.0.

acetone conversion increased by increasing the residence time in zone II. In order to obtain an acetone conversion of, for example, 99.5%, a residence time longer than 18 min was required. This determines the volume of the simulated moving-bed reactor. The results of the numerical simulation of this case were already shown in Fig. 8(a)–(c).

5. Conclusions

The reaction rate of the BPA production from acetone and phenol catalyzed by the proton-type ion-exchange resin was measured in batch reaction experiments. The reaction rate equation was determined under the condition of excess phenol with taking into account the inhibition effect of water. The adsorption isotherms and overall volumetric mass transfer coefficients were measured in batch adsorption and breakthrough experiments. Using the determined parameters, the numerical simulation of the 3-zone-type simulated moving-bed reactor was carried out. As a result, when the liquid–solid velocity ratio was less than 5, water was successfully removed out of the reaction zone to reduce catalytic degradation due to water adsorption. In order to desorb water from the resin, a liquid–solid velocity ratio higher than 20 was required in zone IV. When the flow rates of liquid and resin were set appropriately, the inhibition effect of water became negligible and a long-term stable operation was allowed.

6. Nomenclature

C, C_k	concentration in the liquid phase (mol m^{-3})
C^*, C_k^*	equilibrium concentration to the adsorbed amount (mol m^{-3})
C_0	saturated concentration before the breakthrough experiments (mol m^{-3})
C_1	feed concentration in the breakthrough experiments (mol m^{-3})
C_{A0}	initial concentration of acetone in the batch experiments (mol m^{-3})
K'_A	constant in the reaction rate equation (m^3 mol^{-1})
k_1, k_{-1}	reaction rate constants of elementary reaction Eq. (10)
K_1	$=k_1/k_{-1}$, reaction equilibrium constant of elementary reaction Eq. (10) (m^3 mol^{-1})
k_2, k_{-2}	reaction rate constants of elementary reaction Eq. (11)
$K_f a_v$, $K_f a_{v,k}$	overall volumetric liquid–solid mass transfer coefficient (min^{-1})
k_k, k_{-k}	adsorption and desorption rate constants of component k(=A, D)
K_k	$=k_k/k_{-k}$, adsorption equilibrium constant of component k(=A, D)
k_{m1}	first-order catalytic reaction rate constant (m^3 kg^{-1} s^{-1})
L_a	column length (m)
m_k	adsorption parameter (dimensionless)
n_n	number of columns in zone n (dimensionless)
q, q_k	adsorbed amount (mol m^{-3}-resin)
$r_{k,m}$	catalytic reaction rate of component k (mol kg^{-1} s^{-1})
t	time coordinate (min)
T	temperature (K)
T_S	switching interval (min)
u_n	liquid velocity of the equivalent true moving bed in zone n (m min^{-1})
u_S	solid velocity (m min^{-1})
v, v_n	superficial liquid velocity (m min^{-1})
v_f	liquid velocity calculated from the feed flow rate divided by the cross-sectional area of a column in the simulated moving-bed reactor (m min^{-1})
x_A	acetone conversion (dimensionless)

Y_D	water recovery (dimensionless)
z	distance from the liquid inlet (m)

Greek letters

$\beta_{k,n}$	β parameter of component k in zone n, defined in Eq. (23) (dimensionless)
ϵ_b	bed porosity (dimensionless)
ρ	packing density of the resin (kg m^{-3})
τ_{II}	liquid residence time of the equivalent true moving bed in zone II (min)

Subscripts

A	acetone
B	phenol
C	bisphenol A (BPA)
D	water
f	feed stream in the SMBR experiments
k	component k(=A, C, D)
n	zone n(=II, III, IV)
n_{in}	liquid inlet of zone n
n_{out}	liquid outlet of zone n

Acknowledgements

The authors would like to thank Japan Organo for providing the ion-exchange resins.

References

[1] S. Asaoka, A. Kuguru, K. Ueda, S. Yamamoto, A. Shindo, Jpn. Kokai Tokkyo Koho, 94-340564 (1994).
[2] M. Kawase, T.B. Suzuki, K. Inoue, K. Yoshimoto, K. Hashimoto, Chem. Eng. Sci. 51 (1996) 2971.
[3] M. Mazzotti, A. Kruglov, B. Neri, D. Gelosa, M. Morbidelli, Chem. Eng. Sci. 51 (1996) 1827.
[4] M.T. Shieh, P.E. Barker, J. Chem. Technol. Biotechnol. 63 (1995) 125.
[5] A.K. Ray, R.W. Carr, Chem. Eng. Sci. 50 (1995) 2195.
[6] A.V. Kruglov, M.C. Bjorklund, R.W. Carr, Chem. Eng. Sci. 51 (1996) 2945.
[7] R.A. Reinicker, B.C. Gates, AIChE J. 20 (1974) 933.
[8] P.B. Venuto, P.S. Landis, J. Catal. 6 (1966) 237.
[9] K. Hashimoto, S. Adachi, H. Noujima, H. Maruyama, J. Chem. Eng. Jpn. 16 (1983) 400.
[10] K. Hashimoto, Y. Shirai, M. Morishita, S. Adachi, Kagaku Kogaku Ronbunshu 16 (1990) 193 in Japanese.
[11] K. Hashimoto, S. Adachi, Y. Shirai, M. Morishita, in: G. Ganetsos, P.E. Barker (Eds.), Preparative and Production Scale Chromatography, chapter 13, Marcel Dekker, New York, 1993, p. 273.